Breakdown Characteristics and Mechanisms of Liquid Nitrogen under Transient Thermal Stress for Superconducting Fault Current Limiters

N. Hayakawa, *Member, IEEE,* T. Matsuoka, H. Kojima, *Member, IEEE,* S. Isojima, and M. Kuwata

***Abstract*— We have been investigating the electrical breakdown (BD) characteristics of liquid nitrogen (LN_2) with a transient thermal stresses to simulate the quench conditions of resistive-type superconducting fault current limiters (SFCL). We call such BD of LN_2 with the transient thermal stress as "dynamic BD", and discriminate it from that with a continuous thermal stress. In this paper, we investigated the dynamic BD characteristics of LN_2 for different LN_2 pressures, electrode sizes and terms of transient thermal stress input. In addition, we obtained the BD characteristics of LN_2 with the continuous thermal stress, and compared them with the dynamic BD characteristics. Furthermore, we analyzed the statistical scattering of the time from the thermal stress input to the dynamic BD occurrence and discussed the dynamic BD mechanisms of LN_2. We also proposed a flowchart of rational and reliable electrical insulation design of resistive-type SFCL based on the dynamic BD characteristics of LN_2.**

***Index Terms*— superconducting fault current limiters, quench, liquid nitrogen, bubble, breakdown, insulation design**

I. Introduction

SUPERCONDUCTING fault current limiters (SFCL) are regarded as key devices for reliable power transmission and distribution in a large-capacity and high-density electric network, because SFCL may offer a rapid and effective current limitation at a fault condition. The resistive-type SFCL has been mainly developed and tested around the world [1]–[3]. In order to develop the practical and reliable resistive-type SFCL, electrical breakdown (BD) characteristics of liquid nitrogen (LN_2) under the fault current limiting operation are quite important.

When a quench occurs in the resistive-type SFCL under the fault current limiting operation, a transient thermal stress with bubbles is superposed on a high electric field stress under the operating voltage of SFCL. As the result, the breakdown strength of LN_2 may be reduced, and BD of LN_2 may be induced in the bubble disturbance. Thus, such quench-induced "dynamic BD" characteristics of LN_2 are critical and peculiar to the insulation design of the resistive-type SFCL.

N. Hayakawa, T. Matsuoka, and H. Kojima are with the Department of Electrical Engineering and Computer Science, Nagoya University, Nagoya 464-8603, Japan (e-mail: nhayakaw@nuee.nagoya-u.ac.jp, kojima@nuee.nagoya-u.ac.jp)

S. Isojima is with Sumitomo Electric Industries, Ltd., Osaka 554-0024, Japan (e-mail: isojima-shigeki@sei.co.jp).

M. Kuwata is with Nissin Electric Co., Ltd., Kyoto 615-8686, Japan (e-mail: Kuwata_Minoru@nissin.co.jp)

Most researchers have investigated the BD characteristics of LN_2 with the thermal stress using the continuous thermal stress [4]–[6]. However, the quench and the subsequent bubble disturbance in the resistive-type SFCL are the transient phenomena under the fault current limiting operation. Therefore, the BD characteristics of LN_2 with the continuous thermal stress should be discriminated from those with the transient thermal stress, *i.e.* dynamic BD characteristics of LN_2.

From the above background, we have been investigating the dynamic BD characteristics of LN_2 with the transient thermal stress [7]–[10]. In this paper, we discussed the dynamic BD characteristics and their mechanisms for different LN_2 pressures, electrode sizes and terms of transient thermal stress input. Moreover, in consideration of the dynamic BD characteristics of LN_2, we proposed a flowchart of electrical insulation design of resistive-type SFCL.

II. Experimental Setup and Methods

Figs. 1 and 2 show the experimental setup and the test samples. A high electric field stress and a high thermal stress can be simultaneously applied to the test samples in the cryostat. The cryostat has a FRP capacitor bushing, which is PD free at 150 kV_{rms} in LN_2. The test samples are composed of a high voltage sphere electrode with the diameter ϕ = 6–50 mm and a grounded nichrome sheet electrode with the gap length of 2 mm, *i.e.* under a quasi-uniform electric field with the field utilization factor of 0.950–0.674. The nichrome sheet electrode is used to apply the transient thermal stress with bubbles into the gap space exposed to the high electric field stress. The nichrome sheet is cut into a meander shape with the resistance of 2 Ω in LN_2.

Using the above electrode system, we carried out three kinds of BD tests for different electrode diameters, LN_2 pressures P = 0.1–0.2 MPa at the LN_2 temperature of 77 K [6].

1. *Intrinsic BD test without thermal stress*

   AC high voltage V_a of 60 Hz was applied to the high voltage electrode and increased at 1 kV_{rms}/s until BD occurred in LN_2 without the thermal stress from the nichrome sheet electrode. This test was repeated 20 times and 50% BD voltage ($V_{intrinsic}$) was calculated by the Weibull analysis. $V_{intrinsic}$ was converted to 50% BD electric field strength ($E_{intrinsic}$) at the tip of the sphere electrode.

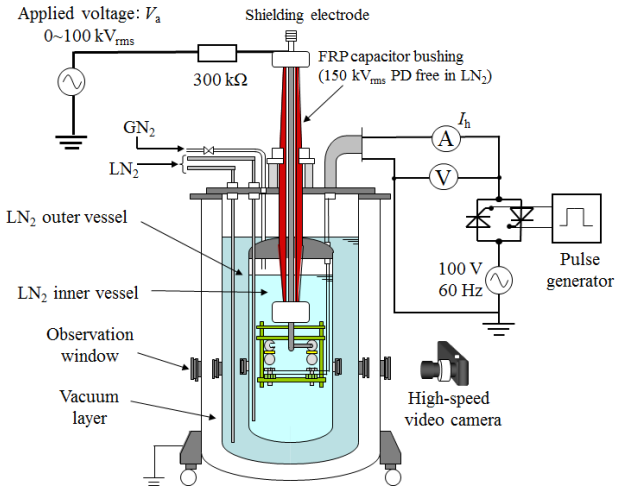

Fig. 1. Experimental setup

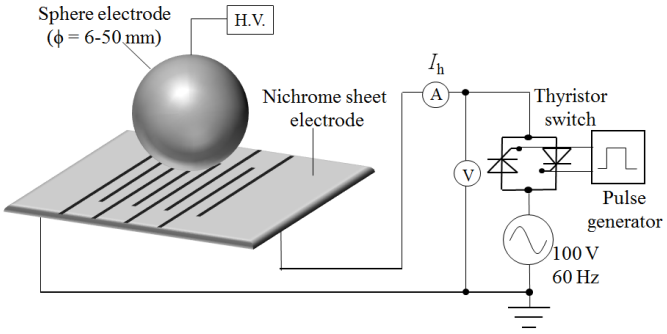

Fig. 2. Test sample configuration

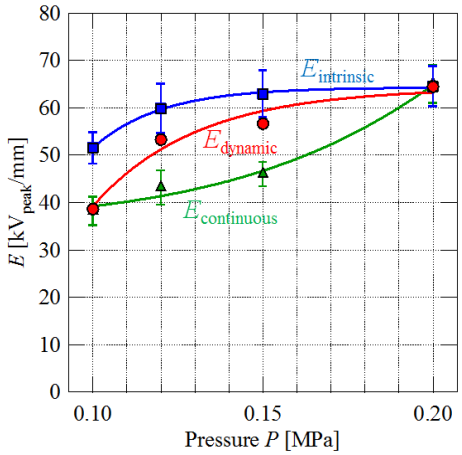

(a) ϕ = 6 mm

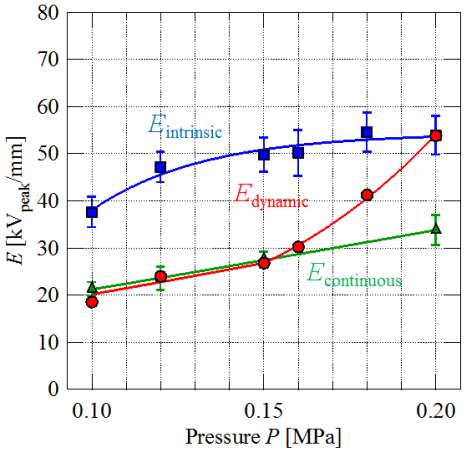

(b) ϕ = 50 mm

Fig. 3. Pressure dependence of BD strength (t_h = 1 s)

2. *BD test with continuous thermal stress*
   After the nichrome sheet electrode was continuously energized with the current I_h = 8 A$_{rms}$, V_a was increased at 1 kV$_{rms}$/s until BD occurred in LN$_2$ under the continuous bubble disturbance. As well as the intrinsic BD test, 50 % BD electric field strength ($E_{continuous}$) was obtained.
3. *Dynamic BD test with transient thermal stress*
   V_a was kept at a constant value below $V_{intrinsic}$. Next, a thermal stress was superposed by energizing the nichrome sheet electrode with I_h = 8 A$_{rms}$ during the term t_h = 0.25–1 s, which is consistent with the ohmic energy level to be generated at the quench of superconducting tapes for SFCL. This test was repeated 20 times at the same V_a and t_h, and counted the number of the dynamic BD occurrence in LN$_2$ to get the BD probability at each V_a. Owing to the linearity between the BD probability and V_a, 50 % BD electric field strength ($E_{dynamic}$) was evaluated.

III. Experimental Results and Discussion

A. Breakdown strength with transient thermal stress

Fig. 3 shows the pressure dependence (P = 0.1–0.2 MPa) of 50% BD electric field strengths $E_{intrinsic}$, $E_{continuous}$ and $E_{dynamic}$ at t_h = 1 s for (a) ϕ = 6 mm and (b) ϕ = 50 mm, respectively. $E_{dynamic}$ increased with the increase in P and approached $E_{intrinsic}$ at P = 0.2 MPa. This is attributed to the reduction of the number and size of bubbles in the pressurized LN$_2$. Thus, the pressurization of LN$_2$ is an effective method to prevent the dynamic BD occurrence in LN$_2$. At $P \geq$ 0.12 MPa for ϕ = 6 mm and at P > 0.15 MPa for ϕ = 50 mm, $E_{dynamic}$ becomes higher than $E_{continuous}$.

Figs. 4 and 5 show the heater energizing time dependence (t_h = 0.25–1 s) of 50% BD electric field strength at ϕ = 6 mm and ϕ = 50 mm, respectively, for different pressures. At $P \geq$ 0.1 MPa for ϕ = 6 mm and at $P \geq$ 0.15 MPa for ϕ = 50 mm, $E_{dynamic}$ increased with the decrease in t_h, and approached $E_{intrinsic}$ at the shorter t_h. $E_{dynamic}$ also approached $E_{continuous}$ at the longer t_h. The electrode diameter dependence of 50% BD electric field strength in Figs. 4 and 5 is attributed to the size effect or the volume effect [6][11], *i.e.* the BD strength decreased with the increase in the electrode diameter with the larger LN$_2$ volume of high electric field strength.

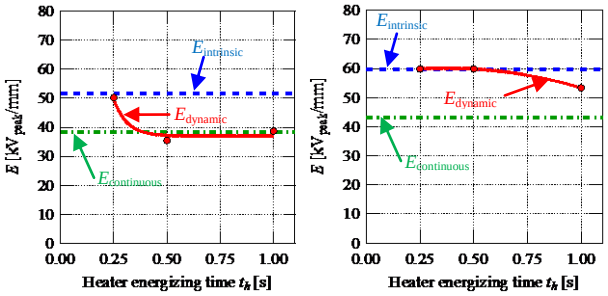

(a) P = 0.10 MPa (b) P = 0.12 MPa

Fig. 4 Heater energizing time dependence of BD strength (ϕ = 6 mm)

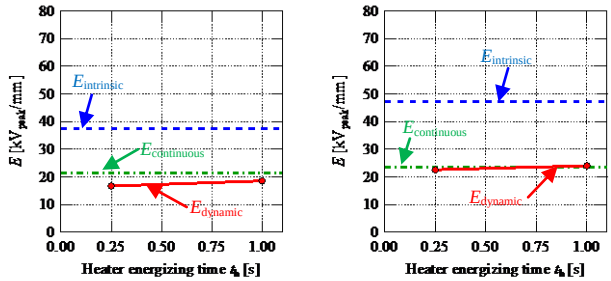

(a) P = 0.10 MPa (b) P = 0.12MPa

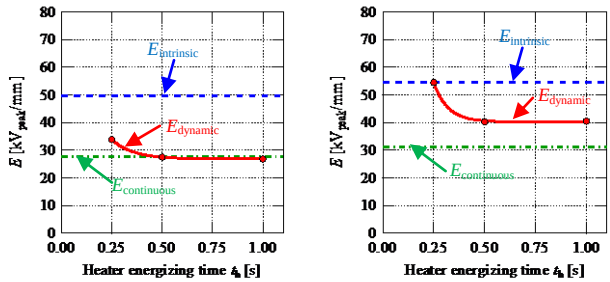

(c) P = 0.15 MPa (d) P = 0.20 MPa

Fig. 5 Heater energizing time dependence of BD strength (ϕ = 50 mm)

B. Discussion on dynamic BD mechanisms

In order to discuss the dynamic BD mechanisms, we focused on the time from the thermal stress input to the dynamic BD occurrence, which is defined as the dynamic BD time t_{BD}. We introduced the Weibull statistics for the evaluation of the statistical scattering of t_{BD}. Fig. 6 shows the Weibull plots of t_{BD} for (a) t_h = 0.25 s and (b) t_h = 1 s, respectively, at ϕ = 50 mm, P = 0.1 MPa and V_a = 35 kV_{peak}. In the case of t_h = 0.25 s, the Weibull plots of t_{BD} are expressed by an approximate line with the inclination (shape parameter) of a = 7.12, which means that the dynamic BD was based on a single mechanism. On the other hand, in the case of t_h = 1 s, the Weibull plots have two shape parameters of a_1 = 10.5 and a_2 = 1.07, which suggests that two different mechanisms are mixed in the dynamic BD.

Fig. 7 shows the shape parameters of t_{BD} for different parameters of ϕ, P, t_h and V_a. The shape parameters of t_{BD}

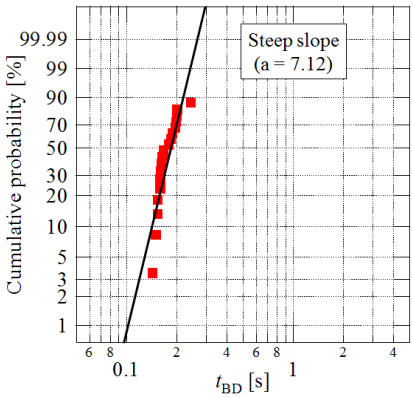

(a) t_h = 0.25 s

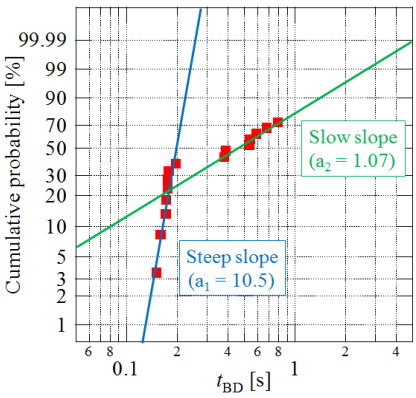

(b) t_h = 1 s

Fig. 6 Weibull plots of t_{BD} (ϕ = 50 mm, P = 0.1 MPa, V_a = 35 kV_{peak})

		Presser P [MPa]							
		0.10	0.12	0.15	0.20	0.10	0.12	0.15	0.20
Electrode diameter ϕ [mm]	Heater energizing time t_h [s]	Steep slope				Slow slope			
6	0.5	◆	-	-	-	-	-	-	-
	1	▲	▲	▲	-	-	△	△	-
20	1	■	■	■	-	□	□	□	-
50	0.25	◀	◀	◀	-	-	-	-	-
	0.5	-	-	⋈	⋈	-	-	-	-
	1	●	●	●	●	○	○	○	○

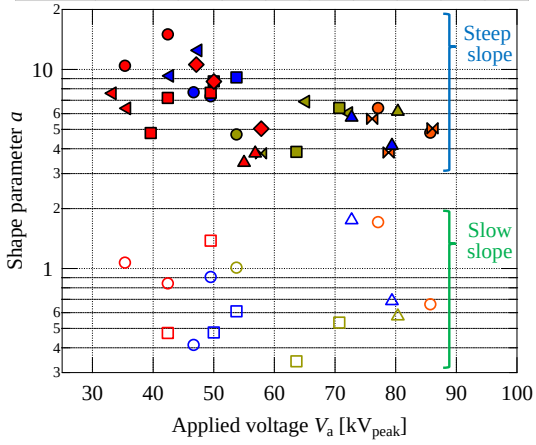

Fig. 7 Shape parameter of t_{BD}

were classified into two categories; $a < 2$ for the slow slope and $a > 3$ for the steep slope. According to the Weibull statistics, $a = 1$ indicates that the failure rate (BD probability) is constant, *i.e.* "random process". On the other hand, $a > 1$ indicates that the failure rate increases with time, *i.e.* "aging process". The dynamic BD with $a < 2$ corresponds to the random process, where the BD probability is almost constant in the bubble disturbance after the LN_2 gap space is filled with the bubbles, similar to the BD with the continuous thermal stress. On the other hand, the dynamic BD with $a > 3$ corresponds to the aging process, where the BD probability increases with time in the transient generation and propagation of bubbles before the LN_2 gap space is filled with the bubbles. The latter BD process with $a > 3$ is peculiar to the dynamic BD under the transient bubble disturbance.

C. Insulation design of resistive-type SFCL

The experimental results in the previous sub-sections mean that the insulation design of resistive-type SFCL based on the BD characteristics of LN_2 with the continuous thermal stress can be considered to be conservative or pessimistic. Therefore, in order to make the most use of the resistive-type SFCL, a rational and reliable insulation design can be expected based on the dynamic BD characteristics of LN_2 with the transient thermal stress.

Fig. 8 shows a flowchart of the insulation design for resistive-type SFCL based on the dynamic BD characteristics. The electric power system concerned with SFCL gives the rated current, voltage and prospective fault current, etc. of SFCL. The fault current limitation design of SFCL will be done with the coil specifications (diameter, length, etc.) and tape specifications (width, critical current, etc.) of SFCL as well as the requirements (limitation rate, fault clearance time, recovery time, etc.) of the power system. The initial or fundamental insulation design of SFCL can be done based on the intrinsic BD characteristics of LN_2 without the thermal stress, which can determine the LN_2 pressure, the gap lengths between the SFCL coils or between the SFCL coil and the grounded tank, etc. Then, supposing the quench occurrence of SFCL at the fault condition, the possibility of dynamic BD occurrence should be discussed, e.g. using the data in Fig. 3. If the dynamic BD can occur, the fault current limitation design and/or insulation design of SFCL should be modified. Such a design and operation scheme of SFCL is expected to be coordinated with the other SFCLs to be introduced in the power system.

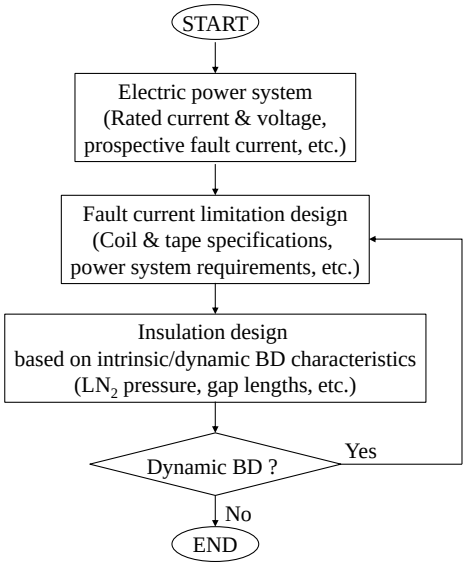

Fig. 8 Flowchart of insulation design for resistive-type SFCL

IV. CONCLUSION

This paper described the BD characteristics and mechanisms of LN_2 for resistive-type SFCL under the fault current limiting operation. The main results can be summarized as follows:

1. Dynamic BD strength $E_{dynamic}$ increased at the shorter heater energizing time t_h and approached the intrinsic BD strength $E_{intrinsic}$. $E_{dynamic}$ decreased at the longer t_h and approached the BD strength $E_{continuous}$ with the continuous thermal stress.
2. Weibull statistics of the time t_{BD} from the thermal stress input to the dynamic BD occurrence suggested that the dynamic BD mechanisms can be classified into two processes; random process and aging process.
3. The insulation design based on $E_{continuous}$ for resistive-type SFCL may be conservative or pessimistic. A rational and reliable insulation design based on $E_{dynamic}$ was proposed with a flowchart.

REFERENCES

[1] H.-P. Kraemer, W. Schmidt, H. Cai, B. Gamble, D. Madura, T. MacDonald, J. McNamara, W. Romanosky, G. Snitchler, N. Lallouet, F. Schmidt, and S. Ahmed., "Superconducting fault current limiter for transmission voltage", *Physics Procedia*, vol.36, pp.921-926, 2012

[2] A. Morandi, "Fault current limiter: an enabler for increasing safety and power quality of distribution networks," *IEEE Trans. Appl. Supercond.*, vol.23, no.6, 5604608, 2013

[3] J. Bock, A. Hobl, J. Schramm, S. Krämer, and C. Jänke, "Resistive superconducting fault current limiters are becoming a mature technology," *IEEE Trans. Appl. Supercond.*, vol.25, no.3, 5600604, 2015

[4] N. Hayakawa, H. Kojima, M. Hanai, and H.Okubo, "Recent progress in electrical insulation techniques for HTS power apparatus," *Physics Procedia*, vol.36, pp.1305–1308, 2012

[5] N. Hayakawa, T. Matsuoka, S. Nishimachi, and H. Kojima, "Quench-induced dynamic breakdown characteristics of LN_2 and LN_2/PPLP composite electrical insulation system for superconducting power apparatus," *IEEE Trans. Appl. Supercond.*, vol.25, no.3, 7700304, 2015

[6] N. Hayakawa, T. Matsuoka, K. Ishida, H. Kojima, S. Isojima, and M. Kuwata, "Pressure dependence and size effect of LN_2 breakdown characteristics under transient thermal stress," *IEEE Trans. Appl. Supercond.*, vol. 26, issue 3, 7700604, 2016

[7] M. Hara, D. J. Kwak, and M. Kubuki, "Thermal bubble breakdown characteristics of LN_2 at 0.1 MPa under a.c. and impulse electric fields," *Cryogenics*, vol.29, pp.895–903, 1989

[8] I. Sauers, R. James, A. Ellis, E. Tuncer, G. Polizos, and M. Pace, "Effect of bubbles on liquid nitrogen breakdown in plane-plane electrode geometry from 100-250 kPa," *IEEE Trans. Appl. Supercond.*, vol.21, no.3, pp.1892–1895, 2011

[9] M. Blaz and M. Kurrat, "Influence of bubbles in pressurized liquid nitrogen on the discharge behavior in a homogeneous electric field," *IEEE Trans. Appl. Supercond.*, vol.23, 7700804, 2013

[10] S. Fink, H.-R. Kim, R. Mueller, M. Noe, and V. Zwecker, "AC breakdown voltage of liquid nitrogen depending on gas bubbles and pressure," *Int. Conf. on High Voltage Engineering and Application (ICHVE)*, 7035445, 2014

[11] N. Hayakawa, S. Nishimachi, H. Kojima, and H.Okubo, "Size Effect on Breakdown Strength in Sub-cooled Liquid Nitrogen for Superconducting Power Apparatus," *IEEE Trans. Dielectr. Electr. Insul.*, vol. 22, no. 5, pp. 2565–2571, 2015